

Measurement of the thickness-dependent magnetic anisotropy of Co/GaAs(001)

X. Y. Xu, L. F. Yin, D. H. Wei, C. S. Tian, G. S. Dong, and X. F. Jin*
 Surface Physics Laboratory, Fudan University, Shanghai 200433, People's Republic of China

Q. J. Jia
 National Synchrotron Radiation Laboratory, Beijing 310027, People's Republic of China
 (Received 6 November 2007; published 6 February 2008)

The structure and magnetic anisotropy of epitaxially grown thin Co films on GaAs(001) are studied as a function of thickness by reflection high energy electron diffraction, x-ray diffraction, and rotating-magneto-optical Kerr effect. The cubic anisotropy constant is determined to be $K_1 = -6.5 \times 10^4$ erg/cm³ for bcc Co, which is in accordance with the anisotropy evolution of bulk Fe_xCo_{1-x} alloy.

DOI: 10.1103/PhysRevB.77.052403

PACS number(s): 75.30.Gw, 75.70.Ak

The correlation between the magnetocrystalline anisotropy and the crystallographic structure for a given single crystalline magnetic material has long been one of the central issues in modern magnetism. It was first predicted by Powell and Fowler that the easy and hard axes of a substance depended primarily only upon the structure,^{1,2} for instance, any ferromagnetic material with body-centered-cubic (bcc) structure would be expected to have $\langle 100 \rangle$ as the easiest directions, or a positive cubic magnetic anisotropy constant K_1 , similar to that of bcc Fe. It was later realized by Shih that this prediction could not be generally valid, because bcc Co_xFe_{1-x} alloys had just the opposite behavior when $0.40 < x < 0.70$, showing $\langle 111 \rangle$ as the easy axes and $\langle 100 \rangle$ the hard axes, corresponding to a negative K_1 .³ For single crystalline thin films, the magnetocrystalline anisotropy is usually determined by the in-plane magnetic anisotropy. For example, the fourfold anisotropy with $\langle 100 \rangle$ as the easy axes has a positive K_1 while that with $\langle 110 \rangle$ as the easy axes corresponds to a negative K_1 for (001) thin films. bcc Co film which does not exist naturally was first obtained by Prinz by epitaxial growth on GaAs(110).⁴ Experimental data showed that $[100]$ was the easy, $[111]$ the intermediate, and $[110]$ the hard axes. This could hardly be explained by either positive or negative K_1 . However, they declared that bcc Co should have a negative K_1 by assuming a strong in-plane uniaxial anisotropy field existing along the Co $[100]$ direction.⁵ Later, Blundell *et al.* found that an in-plane fourfold magnetic anisotropy existed in 4 nm Co/GaAs(001) but with the easy axes along the $\langle 100 \rangle$ directions.⁶ It was further observed by Gu *et al.* that the stable phase in the 5–15 nm Co/GaAs(001) was not bcc but a hexagonal-close-packed (hcp) structure with two domains with the $(\bar{1}2\bar{1}0)$ plane parallel to the GaAs(001). The in-plane magnetic fourfold anisotropy was caused by a superposition of two mutually perpendicular uniaxial contributions corresponding to the two domains ($[0001]\text{Co} \parallel [110]\text{GaAs}$, $[0001]\text{Co} \parallel [\bar{1}\bar{1}0]\text{GaAs}$).^{7,8} In our previous works, we clarified that Co grew on GaAs(001) in three stages: bcc phase during the initial stage for $d_{\text{Co}} < 2$ nm, coexisting bcc and hcp phases in the middle stage for $2 < d_{\text{Co}} < 6$ nm, and then hcp phase for $d_{\text{Co}} > 6$ nm.^{9,10} Meanwhile, a positive in plane fourfold magnetic anisotropy with easy axes along the $\langle 100 \rangle$ directions were inferred from the shapes of magnetic M - H loops for a

2 nm Co film.^{9,11} Theoretically Klautau and Eriksson predicted that the surface layers contributed a large positive K_1 which was different compared to that of bulk bcc Co.¹² Therefore, the fundamental question still remains, whether the cubic magnetocrystalline anisotropy K_1 is positive or negative for bcc Co.

In this work, we found that the issue about magnetic anisotropy of bcc Co on GaAs(001) is actually much more involved than we would have expected. It depends strongly on the film thickness as well as the growth temperature. Here, we use grazing incident x-ray diffraction (GIXRD) and reflection-high-energy electron diffraction (RHEED) to determine the structure of Co on GaAs(001) and rotating-magneto-optic-Kerr-effect (ROTMOKE) technique to determine the magnetocrystalline anisotropy constant.^{13–16} The Co films were deposited on GaAs(001) substrates at different growth temperatures from 60 to 160 °C. Experimental details have been described in our previous works.^{9,10} The films were capped with 3.0 nm Au to prevent oxidation. GIXRD and all the magneto-optic-Kerr-effect (MOKE) measurements were done *ex situ*. In Fig. 1(a), RHEED pattern of 1.2 nm thick Co deposited at 120 °C indicates that the film has a bcc structure since it is similar to that of bcc Fe on GaAs(001).¹³ For the 3 nm thick Co deposited at 120 °C, there appears some additional dots [emphasized in Fig. 1(b) by the ellipse]. These are due to hcp Co.¹⁰ In order to confirm the bcc structure of 1.2 nm Co, we conducted GIXRD measurements [shown in Fig. 1(c)] at the Beijing Synchrotron Radiation Facility at an incident beam angle of 0.2° to the GaAs(001) plane using photon energy of 8.052 keV. The broad peak at 22.3° is due to Au(200) (blue curve). The inset shows the zoomed area (indicated by the rectangle) which shows clearly that the curve is a superposition of two peaks, a sharp and a broad one. The sharp peak at 22.75° corresponds to the GaAs(220) substrate (the magenta curve). The small broad peak at 22.77° (the green curve) is due to bcc Co(110) with a lattice constant of 0.281 nm. Since no signal is observed at the expected hcp Co(1100) peak at 20.8°, the structure of this Co sample is inferred to be pure bcc.

Representative longitudinal-MOKE loops for 1.4 nm bcc Co grown at 120 °C are shown in Fig. 2(a). The easy axis is along Co $[\bar{1}\bar{1}0]$ the hard axis along $[110]$, and $[010]$ the intermediate. Note that the loops only show twofold symmetry

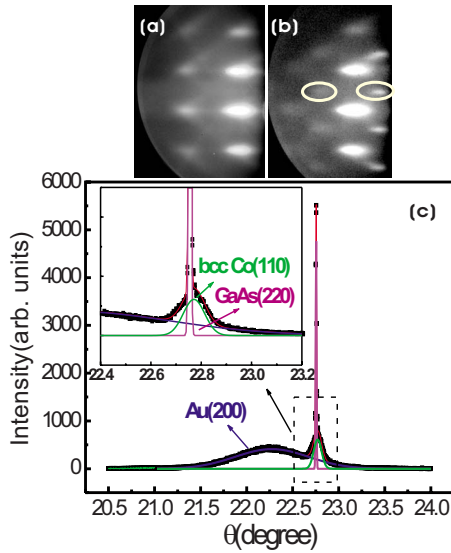


FIG. 1. (Color online) (a) RHEED pattern of 1.2 nm Co deposited at 120 °C on GaAs(001). The electron beam was incident along GaAs[110] direction. (b) RHEED pattern of 3 nm Co deposited at 120 °C on GaAs(001). The dots in the ellipses are from hcp Co. (c) GIXRD of 1.2 nm Co deposited at 120 °C on GaAs(001). The inset is a zoomed in figure of the main peak. Black solid squares are experiment data and solid lines are fitting curves.

implying that the in-plane uniaxial anisotropy plays a dominant role. Therefore, it is difficult to extract the easy axes of the fourfold anisotropy field from the MOKE loops. However, it has been recognized that ROTMOKE is an effective, sensitive, and well defined technique in such uniaxial aniso-

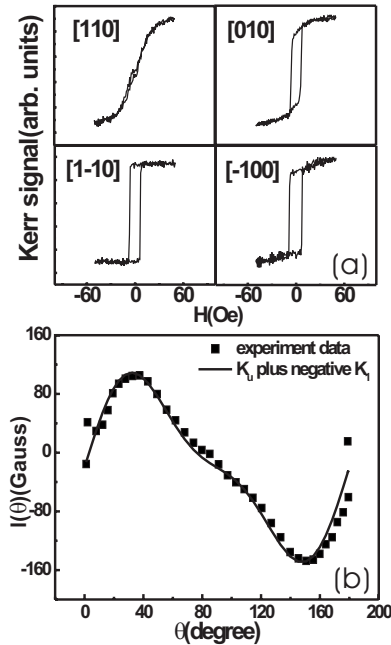


FIG. 2. (a) Longitudinal-MOKE loops and (b) ROTMOKE data of 1.4 nm Co deposited at 120 °C on GaAs(001), $H_{K_1} = -152$ Oe and $H_{K_u} = 220$ Oe. All the MOKE measurements were done at room temperature.

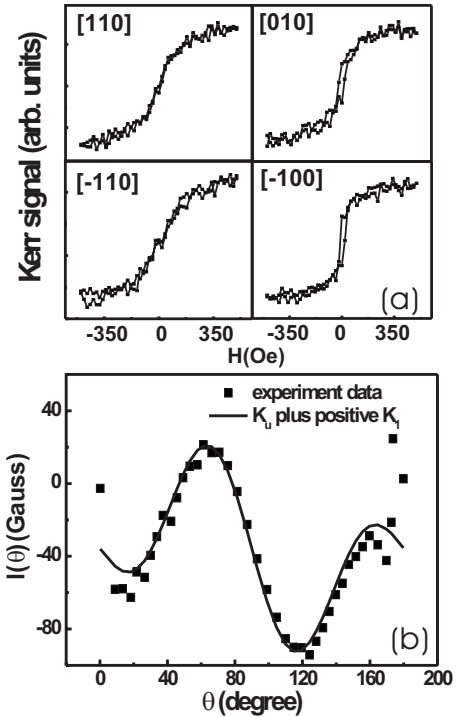


FIG. 3. (a) Longitudinal-MOKE loops and (b) ROTMOKE data of 2.0 nm Co deposited at 160 °C on GaAs(001), $H_{K_u} = 62$ Oe and $H_{K_1} = +132$ Oe.

tropy dominant cases.^{13,15,18} Figure 2(b) shows the ROTMOKE curve for the 1.4 nm thick Co deposited at 120 °C. The solid squares are the torque values as a function of the angle between magnetization and the easy axis. The data were fitted to the equation¹³

$$E/V = -M_s H \cos(\alpha - \phi) + K_u \sin^2 \phi + K_1 \sin^2(\phi + \pi/4) \cos^2(\phi + \pi/4).$$

Here, E is the free energy, V is the volume of the film, M_s is the saturation magnetization, H is the magnetic field, α is the angle between the magnetic field and Co[1 $\bar{1}$ 0], and ϕ is the angle between magnetization and Co[1 $\bar{1}$ 0]. The solid line is a fit to the data with $K_1 < 0$. It is clear that a negative K_1 and a uniaxial field are required to give the best fit. The best fit parameters were determined to be $H_{K_1} = 2K_1/M_s = -152$ Oe and $H_{K_u} = 2K_u/M_s = 220$ Oe. Therefore, although it seems contradictory to our own previous experiment,⁹ we have unambiguously determined that K_1 is negative. The negative anisotropy field means that the easy axes of fourfold anisotropy are along Co \langle 110 \rangle .

A 2.0 nm Co film on GaAs(001) deposited at 160 °C which also showed similar growth condition to that of Wu *et al.*⁹ was also studied. Although weak, the magnetic signal was clear enough to distinguish the easy and hard axes. The longitudinal MOKE loops shown in Fig. 3(a) also have the similar shapes as our previous work reported. The easy axes of the sample were along Co \langle 100 \rangle , while the hard axes were parallel to Co \langle 110 \rangle . The loops indicated a fourfold dominant

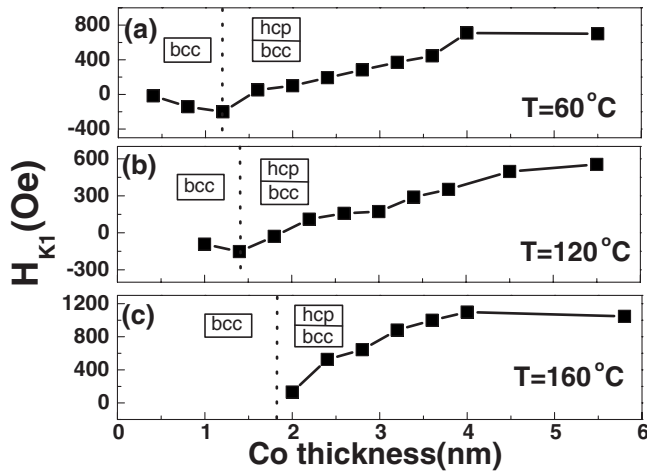


FIG. 4. H_{K_1} vs Co thickness for Co wedge samples grown at (a) 60 °C, (b) 120 °C, and (c) 160 °C. Each H_{K_1} value is fitted from ROTMOKE experiment. The dashed line denotes the structure phase transition thickness.

anisotropy, which corresponded to a positive K_1 . Figure 3(b) shows the torque values measured by ROTMOKE. As before, the fits were done according to the equation given above. It is clear that the best fit is given with $K_1 > 0$ (solid line). The fit parameters gave H_{K_1} as +132 Oe and a comparatively smaller uniaxial anisotropy field of 62 Oe.

The difference between the two samples which have the opposite sign of magnetocrystalline anisotropy is puzzling because both seem to be in the bcc phase according to the RHEED pattern. To investigate this point, a systematic study of the anisotropy as a function of the growth temperature and thickness was investigated. Figure 4 shows the fourfold anisotropy H_{K_1} vs film thickness for different growth temperatures, 60, 120, and 160 °C. There exists a structural phase transition from bcc to hcp for the films. The transition thickness is different for the different temperatures and are indicated by the dashed line. It was observed that the structural transition thickness for deposition temperature of 150 °C was 2.0 nm.^{9,10} In Fig. 4(a), the fourfold anisotropy fields for Co thinner than 1.2 nm deposited at 60 °C are negative and the absolute values increase monotonically with thickness, suggesting the bulklike origin of the fourfold anisotropy. If the fourfold anisotropy is from the surface anisotropy, it would decrease with the thickness. When the Co is thicker than 1.2 nm, the absolute values first decrease to zero at 1.8 nm and then increase with increasing thickness. Above 1.2 nm, hcp Co develops on top of bcc Co.^{10,17} It was pointed out by Gu *et al.* that the fourfold anisotropy constant contributed by hcp Co was positive.⁷ This positive contribution conceals the negative anisotropy field of the bcc Co and dominates as the thickness increases. As Fig. 4(b) shows, the Co film grown at 120 °C also has negative K_1 below 1.4 nm and as the thickness is increased, K_1 becomes positive. For a substrate temperature of 160 °C, no negative H_{K_1} is observed [Fig. 4(c)]. At or above 160 °C, although bcc Co is more easily obtained, the reaction between Co and GaAs substrate is more severe, which results in the nonmagnetic bcc CoGaAs compound. No Kerr signal was detected for

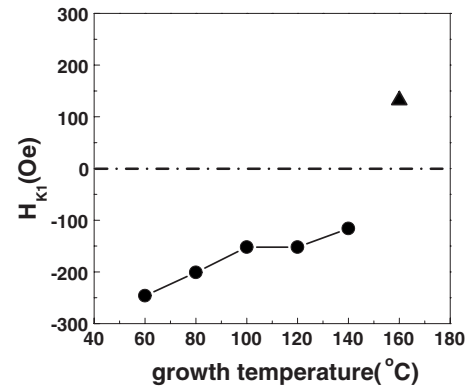


FIG. 5. Fourfold anisotropy field vs growth temperature. Dots are fourfold anisotropy field at the transition Co thickness. For Co grown at 160 °C, there is no transition point. Triangle is the first measurable point, which has a positive K_1 .

thicknesses below 2.0 nm Co. Longitudinal-MOKE loops of the 2.0 nm Co deposited at 160 °C are similar to those of our previous work showing fourfold symmetric loops with the easy axis along Co $\langle 100 \rangle$.⁹

Three other series of samples with growth temperatures of 80, 100, and 140 °C were also investigated. H_{K_1} for these samples also shows the same trend as in Fig. 4. Samples thinner than the structure transition thickness show negative H_{K_1} . Figure 5 shows the temperature dependence of the fourfold anisotropy field at the transition thicknesses. All the samples in the growth temperature range of 60–140 °C have negative H_{K_1} , which decreases as the growth temperature increases. The reason is that the effective magnetic bcc Co thickness decreases as the temperature is increased. Above 160 °C, no transition can be found. The triangle (positive H_{K_1}) is the first measurable magnetic signal which arises due to hcp Co. Thus, the proper temperature to prepare the magnetic bcc Co is below 160 °C.

In summary, we have investigated the fourfold anisotropy field of bcc Co as well as hcp Co at a series of growth temperatures. The easy axes of the fourfold anisotropy of bcc Co aligns along Co $\langle 110 \rangle$. By comparison, the easy axes of magnetocrystalline anisotropy for Fe on GaAs(001) are along Fe $\langle 100 \rangle$ directions.^{13,19} For the 1.4 nm bcc Co film (120 °C), $H_{K_1} = -152$ Oe and $H_{K_u} = 220$ Oe. The literature value of magnetic moment of bcc Co was $1.53\mu_B$.⁴ Then, $K_1 = H_{K_1} M_s / 2 = -6.5 \times 10^4$ erg/cm³. For hcp Co, K_1 is positive. The fourfold anisotropy of the Co films grown below 160 °C switches from negative to positive depending on the Co thickness. The reaction between Co and GaAs would not change the magnetic properties of bcc Co but reduces the effective magnetic bcc Co thickness, which reaches zero when the growth temperature is as high as 160 °C.

This work was supported by the National Natural Science Foundation of China, the 973 Project under Grant No. 2006CB921303 of the Science and Technology Ministry of China, the Ministry of Education of China for Ph.D. Training, and the Shanghai Science and Technology Committee.

*Corresponding author; xfjin@fudan.edu.cn

- ¹F. C. Powell, Proc. R. Soc. London, Ser. A **130**, 167 (1930).
- ²R. H. Fowler and F. C. Powell, Proc. Cambridge Philos. Soc. **27**, 280 (1931).
- ³J. W. Shih, Phys. Rev. **46**, 139 (1934).
- ⁴G. A. Prinz, Phys. Rev. Lett. **54**, 1051 (1985).
- ⁵X. Liu, R. L. Stamps, R. Sooryakumar, and G. A. Prinz, Phys. Rev. B **54**, 11903 (1996).
- ⁶S. J. Blundell, M. Gester, J. A. C. Bland, C. Daboo, E. Gu, M. J. Baird, and A. J. R. Ives, J. Appl. Phys. **73**, 5948 (1993).
- ⁷E. Gu, M. Gester, R. J. Hicken, C. Daboo, M. Tselepi, S. J. Gray, J. A. C. Bland, L. M. Brown, T. Thomson, and P. C. Riedi, Phys. Rev. B **52**, 14704 (1995).
- ⁸T. L. Monchesky and J. Unguris, Phys. Rev. B **74**, 241301(R) (2006).
- ⁹Y. Z. Wu, H. F. Ding, C. Jing, D. Wu, G. L. Liu, V. Gordon, G. S. Dong, X. F. Jin, S. Zhu, and K. Sun, Phys. Rev. B **57**, 11935 (1998).
- ¹⁰Y. Z. Wu, H. F. Ding, C. Jing, D. Wu, G. S. Dong, X. F. Jin, K. Sun, and S. Zhu, J. Magn. Magn. Mater. **198**, 297 (1998).
- ¹¹N. A. Morley, M. R. J. Gibbs, E. Ahmad, I. G. Will, and Y. B. Xu, J. Phys.: Condens. Matter **18**, 8781 (2006).
- ¹²A. B. Klautau and O. Eriksson, Phys. Rev. B **72**, 014459 (2005).
- ¹³Z. Tian, C. Tian, L. Yin, D. Wu, G. Dong, X. Jin, and Z. Qiu, Phys. Rev. B **70**, 012301 (2004).
- ¹⁴R. Mattheis and G. Quednau, J. Magn. Magn. Mater. **205**, 143 (1999).
- ¹⁵C. S. Tian, D. Qian, D. Wu, R. H. He, Y. Z. Wu, W. X. Tang, L. F. Yin, Y. S. Shi, D. S. Dong, X. F. Jin *et al.*, Phys. Rev. Lett. **94**, 137210 (2005).
- ¹⁶L. F. Yin, D. H. Wei, N. Lei, L. H. Zhou, C. S. Tian, G. S. Dong, X. F. Jin, L. P. Guo, Q. J. Jia, and R. Q. Wu, Phys. Rev. Lett. **97**, 067203 (2006).
- ¹⁷M. A. Mangan, G. Spanos, T. Ambrose, and G. A. Prinz, Appl. Phys. Lett. **75**, 346 (1999).
- ¹⁸W. X. Tang, D. Qian, D. Wu, Y. Z. Wu, G. S. Dong, X. F. Jin, S. M. Chen, X. M. Jiang, X. X. Zhang, and Z. Zhang, J. Magn. Magn. Mater. **240**, 404 (2002).
- ¹⁹J. J. Krebs, B. T. Jonker, and G. A. Prinz, J. Appl. Phys. **61**, 2596 (1987).